

Finite-Size Effects and Scaling for the Thermal QCD Deconfinement Phase Transition within the Exact Color-Singlet Partition Function

M. Ladrem and A. Ait-El-Djoudi

Laboratoire de Physique des Particules et Physique Statistique

Ecole Normale Supérieure-Kouba,

B.P. 92, 16050, Vieux-Kouba, Algiers, Algeria.

E-mail: Ladrem@eepad.dz, Aitamel@eepad.dz

(Dated: August 9, 2018)

Abstract.

We study the finite-size effects for the thermal QCD Deconfinement Phase Transition (DPT), and use a numerical finite size scaling analysis to extract the scaling exponents characterizing its scaling behavior when approaching the thermodynamic limit ($V \rightarrow \infty$). For this, we use a simple model of coexistence of hadronic gas and color-singlet Quark Gluon Plasma (QGP) phases in a finite volume. The Color-Singlet Partition Function (CSPF) of the QGP cannot be exactly calculated and is usually derived within the saddle point approximation. When we try to do calculations with such an approximate CSPF, a problem arises in the limit of small temperatures and/or volumes ($VT^3 \ll 1$), requiring then additional approximations if we want to carry out calculations. We propose in this work a new method for an accurate calculation of any quantity of the finite system, without explicitly calculating the CSPF itself and without any approximation. By probing the behavior of some useful thermodynamic response functions on the whole range of temperature, it turns out that in a finite size system, all singularities in the thermodynamic limit are smeared out and the transition point is shifted away. A numerical finite size scaling analysis of the obtained data allows us to determine the scaling exponents of the QCD DPT. Our results expressing the equality between their values and the space dimensionality is a consequence of the singularity characterizing a first order phase transition and agree very well with the predictions of other FSS theoretical approaches and with the results of both lattice QCD and Monte Carlo models calculations.

1. INTRODUCTION

It is generally believed that at sufficiently high temperatures and/or densities a new phase of matter called the Quark Gluon Plasma (QGP) can be created. This is logically a consequence of the quark-parton level of the matter structure and of the dynamics of strong interactions described by the Quantum Chromodynamics (QCD) theory. Its existence, however, has been partly supported by lattice QCD calculations and the Cosmological Standard Model predictions. The only available way it seems to study experimentally the QCD Deconfinement Phase Transition (DPT) is to try to create in Ultra-Relativistic Heavy Ion Collisions (URHIC) conditions similar to those in the early moments of the Universe, right after the Big Bang. If ever the QGP is created in URHIC, the volume within which the eventual formation would take place would certainly be finite. Also, in lattice QCD studies, the scale of the lattice space volume is finite. This motivates the study of the Finite Size Effects (FSE) on the expected DPT from a Hadronic Gas (HG) phase to a QGP phase. These effects are certainly important since statistical fluctuations in a finite volume may hinder a sharp transition between the two phases. Phase transitions are known to be infinitely sharp, signaled by some singularities, only in the thermodynamic limit [1]. In general, FSE lead to a rounding of these singularities as pointed out in [2, 3]. However, even in a such situation, it is possible to obtain informations on the critical behavior. Large but finite systems show a *universal* behavior called “Finite-Size Scaling” (FSS), allowing the put of all the physical systems undergoing a phase transition in a certain number of universality classes. The systems in a given universality class display the same critical behavior, meaning that certain dimensionless quantities have the same values for all these systems. *Critical exponents* are an example of these universal quantities.

In the present work, we study the finite size behavior for the thermally driven QCD DPT. For this purpose, we consider a simple Phase Coexistence Model (PCM) used in [4], in which the mixed phase system has a finite volume: $V = V_{HG} + V_{QGP}$. The parameter \mathfrak{h} representing the fraction of volume occupied by the HG: $V_{HG} = \mathfrak{h}V$, is then defined and can be considered as an order parameter for the QCD DPT. Assuming non-interacting phases (separability of the energy spectra of the two phases), and using the PCM, the total partition function of the system can be written as:

$$Z(\mathfrak{h}) = Z_{QGP}(\mathfrak{h})Z_{HG}(\mathfrak{h})Z_{Vac}(\mathfrak{h}), \quad (1)$$

where:

$$Z_{Vac}(T, \mathfrak{h}) = \exp(-BV_{QGP}/T) = \exp(-BV(1 - \mathfrak{h})/T), \quad (2)$$

accounts for the confinement of the color charge by the real vacuum pressure exerted on the perturbative vacuum (B) of the bag models.

The mean value of any thermodynamic quantity of the system $\langle A(T, \mu, V) \rangle$, as defined in [4], can then be calculated by:

$$\langle A(T, \mu, V) \rangle = \frac{\int_0^1 \mathcal{A}(\mathfrak{h}, T, \mu, V) Z(\mathfrak{h}) d\mathfrak{h}}{\int_0^1 Z(\mathfrak{h}) d\mathfrak{h}}, \quad (3)$$

where $\mathcal{A}(\mathfrak{h}, T, \mu, V)$ is the total thermodynamic quantity in the state \mathfrak{h} , given in the case of an extensive quantity by:

$$\mathcal{A}(\mathfrak{h}, T, \mu, V) = \mathcal{A}_{HG}(T, \mu, \mathfrak{h}V) + \mathcal{A}_{QGP}(T, \mu, (1 - \mathfrak{h})V), \quad (4)$$

and in the case of an intensive quantity, by:

$$\mathcal{A}(\mathfrak{h}, T, \mu, V) = \mathfrak{h}\mathcal{A}_{HG}(T, \mu, \mathfrak{h}V) + (1 - \mathfrak{h})\mathcal{A}_{QGP}(T, \mu, (1 - \mathfrak{h})V), \quad (5)$$

with \mathcal{A}_{QGP} and \mathcal{A}_{HG} the contributions relative to the individual QGP and HG phases, respectively.

We think that the PCM used in our present work is not a characteristic signature in a finite volume which anticipates the behavior of a first order phase transition in the TL. It is well known that finite size effects lead to a non obvious order of the phase transition. A characteristic feature of a truly first order transition in the TL can then appear in the second order transition when the volume of the system is finite and vice versa, and this is considered as a finite size artifact. For example, the phenomenon of coexistence of phases can appear in a truly second order phase transition when the volume of the system is finite, and we can also have a divergent correlation length in a truly first order phase transition [5]. Certainly, these non-characteristic features must disappear when approaching the TL.

For the HG phase, we have considered just pionic degrees of freedom, and the partition function for such a system is simply given by:

$$Z_{HG} = e^{\frac{\pi^2}{30}T^3 V_{HG}}. \quad (6)$$

For the QGP phase, we have considered a free gas of quarks and gluons with the exact color-singletness requirement. The color-singlet partition function of the QGP derived using the group theoretical projection technique formulated by Turko and Redlich [6] can not be exactly calculated and is usually calculated within the saddle point approximation in the limit $V_{QGP}T^3 \gg 1$ as in [7, 8, 9]. It turns out that the use of the obtained approximated partition function for the calculation of a mean value within the definition (3), has as a consequence the absence of the DPT [10]. This is due to the fact that the approximation used for the calculation of the color-singlet partition function breaks down at $V_{QGP}T^3 \ll 1$, and this limit is attained in our case. This has been emphasized in further works in which additional approximations have been used to carry out calculations, as in [4, 8]. We propose in the following a new method which allows us to accurately calculate physical quantities describing well the QCD DPT at finite volumes, avoiding then the problem arising at $V_{QGP}T^3 \ll 1$ and without any approximation. We proceed by using the exact definition of the color-singlet partition function for Z_{QGP} , without explicitly calculating it, in the definition (3) of the mean value of a physical quantity. A first analytical step in the calculation of the mean value is then achieved, and an expression with integral coefficients is obtained. The double integrals are then carried out with a suitable numerical method at each value of temperature and volume, and the behavior of the physical quantity of the finite system can so be obtained on the whole range of temperature, for various volumes, without any restriction. Afterwards, scaling critical exponents characterizing the scaling behavior of some quantities are determined using a numerical FSS analysis.

2. EXACT COLOR-SINGLET PARTITION FUNCTION OF THE QGP

The exact partition function for a color-singlet QGP contained in a volume V_{QGP} , at temperature T and quark chemical potential μ , is determined by [7]:

$$Z_{QGP}(T, V_{QGP}, \mu) = \frac{8}{3\pi^2} \int_{-\pi}^{+\pi} \int_{-\pi}^{+\pi} d\left(\frac{\varphi}{2}\right) d\left(\frac{\psi}{3}\right) M(\varphi, \psi) \tilde{Z}(T, V_{QGP}, \mu; \varphi, \psi), \quad (7)$$

$M(\varphi, \psi)$ is the weight function (Haar measure) given by:

$$M(\varphi, \psi) = \left(\sin\left(\frac{1}{2}(\psi + \frac{\varphi}{2})\right) \sin\left(\frac{\varphi}{2}\right) \sin\left(\frac{1}{2}(\psi - \frac{\varphi}{2})\right) \right)^2, \quad (8)$$

and \tilde{Z} the generating function defined by:

$$\tilde{Z}(T, V_{QGP}, \mu; \varphi, \psi) = Tr \left[\exp \left(-\beta \left(\hat{H}_0 - \mu \left(\hat{N}_q - \hat{N}_{\bar{q}} \right) \right) + i\varphi \hat{I}_3 + i\psi \hat{Y}_8 \right) \right], \quad (9)$$

where $\beta = \frac{1}{T}$ (with the units chosen as: $k_B = \hbar = c = 1$), \hat{H}_0 is the free quark-gluon Hamiltonian, \hat{N}_q ($\hat{N}_{\bar{q}}$) denotes the (anti-) quark number operator, and \hat{I}_3 and \hat{Y}_8 are the color ‘‘isospin’’ and ‘‘hypercharge’’ operators respectively. Its final expression, in the massless limit, can be put on the form:

$$Z_{QGP}(T, V_{QGP}, \mu) = \frac{4}{9\pi^2} \int_{-\pi}^{+\pi} \int_{-\pi}^{+\pi} d\varphi d\psi M(\varphi, \psi) e^{V_{QGP} T^3 g(\varphi, \psi, \frac{\mu}{T})}, \quad (10)$$

with:

$$g(\varphi, \psi, \frac{\mu}{T}) = \frac{\pi^2}{12} \left(\frac{21}{30} d_Q + \frac{16}{15} d_G \right) + \frac{\pi^2}{12} \frac{d_Q}{2} \sum_{q=r,b,g} \left\{ -1 + \left(\frac{(\alpha_q - i(\frac{\mu}{T}))^2}{\pi^2} - 1 \right)^2 \right\} - \frac{\pi^2}{12} \frac{d_G}{2} \sum_{g=1}^4 \left(\frac{(\alpha_g - \pi)^2}{\pi^2} - 1 \right)^2, \quad (11)$$

$d_Q = 2N_f$ and $d_G = 2$ being the degeneracy factors of quarks and gluons respectively, α_q ($q = r, b, g$) the angles determined by the eigenvalues of the color charge operators in eq. (9):

$$\alpha_r = \frac{\varphi}{2} + \frac{\psi}{3}, \quad \alpha_g = -\frac{\varphi}{2} + \frac{\psi}{3}, \quad \alpha_b = -\frac{2\psi}{3}, \quad (12)$$

and α_g ($g = 1, \dots, 4$) being:

$$\alpha_1 = \alpha_r - \alpha_g, \quad \alpha_2 = \alpha_g - \alpha_b, \quad \alpha_3 = \alpha_b - \alpha_r, \quad \alpha_4 = 0. \quad (13)$$

3. FINITE-SIZE EFFECTS

To study the effects of volume finiteness on the thermal QCD DPT within the PCM, we'll examine in the following the behavior of some thermodynamic quantities of the system with temperature, at a vanishing chemical potential ($\mu = 0$), considering the two lightest quarks u and d ($N_f = 2$), and using the common value $B^{1/4} = 145 MeV$ for the bag constant.

The first quantity of interest for our study is the order parameter, which can be simply in this case considered as represented by the hadronic volume fraction. According to (3), its mean value is expressed as:

$$\langle \mathfrak{h}(T, V) \rangle = 1 - \frac{\int_{-\pi}^{+\pi} \int_{-\pi}^{+\pi} d\varphi d\psi M(\varphi, \psi) \int_0^1 \mathfrak{q} e^{\mathfrak{q} \mathfrak{R}(\varphi, \psi; T, V)} d\mathfrak{q}}{\int_{-\pi}^{+\pi} \int_{-\pi}^{+\pi} d\varphi d\psi M(\varphi, \psi) \int_0^1 e^{\mathfrak{q} \mathfrak{R}(\varphi, \psi; T, V)} d\mathfrak{q}}, \quad (14)$$

with: $\mathfrak{R}(\varphi, \psi; T, V) = \left(g_{\mu=0}(\varphi, \psi) - \frac{\pi^2}{30} - \frac{B}{T^4} \right) VT^3$. After integration on the \mathbf{q} variable, the order parameter can be written as:

$$\langle \mathfrak{h}(T, V) \rangle = \frac{L_{01} + L_{02} - L_{12}}{L_{01} - L_{11}}, \quad (15)$$

where the general form of the integral terms appearing in this expression is:

$$L_{nm} = \int_{-\pi}^{+\pi} \int_{-\pi}^{+\pi} d\varphi d\psi M(\varphi, \psi) \frac{(e^{\mathfrak{R}(\varphi, \psi; T, V)})^n}{(\mathfrak{R}(\varphi, \psi; T, V))^m}. \quad (16)$$

These integrals are then carried out using a suitable numerical method at each fixed temperature and volume.

The second quantity of interest is the energy density $\varepsilon(T, V)$, whose mean value is related to $\langle \mathfrak{h}(T, V) \rangle$ by:

$$\langle \varepsilon(T, V) \rangle = e_{HG} + (B - e_{HG})(1 - \langle \mathfrak{h}(T, V) \rangle) - 3T^4 \frac{\tilde{L}_{11} - \tilde{L}_{12} + \tilde{L}_{02}}{L_{01} - L_{11}}, \quad (17)$$

where the new integrals on φ and ψ , noted \tilde{L}_{nm} , are given by:

$$\tilde{L}_{nm} = \int_{-\pi}^{+\pi} \int_{-\pi}^{+\pi} d\varphi d\psi M(\varphi, \psi) g_{\mu=0}(\varphi, \psi) \frac{(e^{\mathfrak{R}(\varphi, \psi; T, V)})^n}{(\mathfrak{R}(\varphi, \psi; T, V))^m}, \quad (18)$$

and: $e_{HG} = \frac{\pi^2}{10} T^4$.

We can also examine the effects of volume finiteness by illustrating two more quantities representing the first derivatives of the two previous ones, i. e., the susceptibility χ defined as:

$$\chi(T, V) = \frac{\partial \langle \mathfrak{h}(T, V) \rangle}{\partial T}, \quad (19)$$

and the specific heat density $c(T, V)$ defined as:

$$c(T, V) = \frac{\partial \langle \varepsilon(T, V) \rangle}{\partial T}. \quad (20)$$

Our results for the variations of these four response functions with temperature at different system sizes are presented in the plots on Figs. (1) and (2) and show a pronounced size dependence over almost the entire temperature range. The curves show that in the limit of an infinite volume, both $\langle \mathfrak{h} \rangle$ and $\frac{\langle \varepsilon \rangle}{T^4}$ exhibit a finite sharp discontinuity, which is related to the latent heat of the DPT, at a bulk transition temperature $T_c(\infty) \simeq 104.35 MeV$, reflecting the first order character of the transition. The quantity $\frac{\langle \varepsilon \rangle}{T^4}$ is traditionally interpreted as a measure of the number of effective degrees of freedom; the temperature increase causes then a ‘‘melting’’ of the constituent degrees of freedom ‘‘frozen’’ in the hadronic state, making the energy density attain its plasma value. This finite discontinuity can be mathematically described by a step function, which transforms to a δ -function in χ and c . When the volume decreases, the four quantities vary continuously such that the finite sharp jump is rounded off and the δ -peaks are smeared out into finite peaks over a range of temperature $\delta T(V)$. This is due to the finite probability of presence of the QGP phase below T_c and of the hadron phase above T_c , induced by the considerable thermodynamical fluctuations.

Another feature which can be noted is that the maxima of these rounded peaks occur at effective transition temperatures $T_c(V)$ shifted away from the bulk transition temperature for infinite volume $T_c(\infty)$. This shift is a consequence of the color-singletness requirement since the effective number of internal degrees of freedom for a color-singlet QGP is drastically reduced with decreasing volume, as it can clearly be seen from the curves and as it has been shown in [7]. Thus, the pressure of the QGP phase is lower at a given temperature, and the mechanical Gibbs equilibrium between the two phases would then be reached for $T_c(V) > T_c(\infty)$.

It can also be noted that, for decreasing volume, while the height of the peak decreases, its width gets larger. To see this in more details, we illustrate in the following the second derivative of the order parameter $\langle \mathfrak{h}(T, V) \rangle'' = \frac{\partial^2 \langle \mathfrak{h}(T, V) \rangle}{\partial T^2}$, which reaches its extrema at temperatures $T_1(V)$ and $T_2(V)$. The width of the transition region can simply be defined by the gap between these two temperatures, i. e., $\delta T(V) = T_2(V) - T_1(V)$. The variations of $\langle \mathfrak{h}(T, V) \rangle''$ with temperature for various sizes are illustrated in Fig. (3), from which it can clearly be seen that the gap between the two extrema decreases with increasing volume.

Finally from the obtained results for the finite size response functions, four finite size effects can be observed:

- the rounding effect of the discontinuities
- the smearing effect of the singularities
- the shifting effect of the transition point
- the broadening effect of the transition region,

and to study quantitatively the volume dependence of these effects, a numerical scaling analysis is carried out, which will be presented in the next section.

4. FINITE-SIZE SCALING ANALYSIS

4.1. Finite-Size Scaling

In statistical mechanics, it is known that only in the thermodynamic limit are phase transitions characterized by the appearance of singularities in some second derivatives of the thermodynamic potential, such as the susceptibility and the specific heat. For a first order phase transition, the divergences are δ -function singularities, corresponding to the finite discontinuities in the first derivatives of the thermodynamic potential, while for a second order phase transition the singularity has a power-law form. For the thermal QCD DPT studied in this work, δ -singularities appear in the susceptibility χ and in the specific heat density c at the thermodynamic limit. In finite volumes, these δ -functions are found to be smeared out into finite peaks. To the finite size effects, four useful characteristic quantities can be associated as illustrated on Fig. (4), which are the maxima of the peaks of the susceptibility $\chi_T^{\max}(V)$ and the specific heat density $c_T^{\max}(V)$, the shift of the transition temperature $\tau_T(V) = T_c(V) - T_c(\infty)$ and the width of the transition region $\delta T(V)$. Each of these quantities can be considered as a signature which may anticipate the behavior in the thermodynamic limit, and is expected to present a scaling behavior described by a power law of the volume characterized by a *Scaling Critical Exponent*. For a first order phase transition, the set of power laws is:

$$\left\{ \begin{array}{l} \chi_T^{\max}(V) \sim V^\gamma \\ c_T^{\max}(V) \sim V^\alpha \\ \delta T(V) \sim V^{-\theta} \\ \tau_T(V) = T_c(V) - T_c(\infty) \sim V^{-\lambda} \end{array} \right. , \quad (21)$$

and it has been shown in the FSS theory [11, 12, 13] that in this case, the scaling exponents θ , λ , α and γ are all equal to unity, and it is only the dimensionality which controls the finite size effects.

At a second order phase transition, the correlation length diverges as: $\xi \propto |T - T_c|^{-\nu}$, and then we predict the same power law behavior as for a first order transition, but with different scaling critical exponents, usually given as:

$$\left\{ \begin{array}{l} \chi_T^{\max}(V) \sim V^{\gamma/\nu} \\ c_T^{\max}(V) \sim V^{\alpha/\nu} \\ \delta T(V) \sim V^{-1/\nu} \\ \tau_T(V) = T_c(V) - T_c(\infty) \sim V^{-1/\nu} \end{array} \right. . \quad (22)$$

The values of the scaling critical exponents may then give an indication on the order of a PT and are usually used as a criterion for the determination of this latter [5, 14].

4.2. Numerical Determination of the Scaling Critical Exponents for the Thermal DPT

In the following, we use a FSS analysis to recover the scaling exponents θ , λ , α and γ for the thermally driven DPT. For this purpose, we proceed by studying the behavior of the response-function maxima, their rounding as well as the shift of the effective transition temperature with varying volume. Let's note that the determination of the location of the maxima of the finite size peaks as well as their heights is done in a numerical way, and this yields a systematic error, which is estimated and given for the determined scaling exponents.

4.2.1. Susceptibility, Specific Heat and Smearing Scaling Exponents

The data of the maxima of the rounded peaks of the susceptibility $|\chi_T|^{\max}(V)$ and the specific heat density $c_T^{\max}(V)$ are plotted versus volume in Figs. (5-left) and (5-right) respectively, and their linearity with V can clearly be noted. A numerical parametrization with the power-law forms: $|\chi_T|^{\max}(V) \sim V^\gamma$ and: $c_T^{\max}(V) \sim V^\alpha$, gives the values of the susceptibility scaling exponent: $\gamma = 1.01 \pm 0.03$, and the specific heat scaling exponent: $\alpha = 1.007 \pm 0.031$, where the associated errors are systematic ones.

Fig. (6) illustrates the plot of the results of the width $\delta T(V)$ with the inverse of the volume, and their fit to the power law form: $\delta T(V) \sim V^{-\theta}$. The obtained smearing scaling exponent is: $\theta = 1.03 \pm 0.03$.

4.2.2. The Shift Scaling Exponent

For the study of the shift of the transition temperature $\tau_T(V) = T_c(V) - T_c(\infty)$, we need to locate the effective transition temperature in a finite volume $T_c(V)$. A way to define $T_c(V)$ is as being the location of the maxima of the rounded peaks of the susceptibility and the specific heat, shifted away from the true transition temperature $T_c(\infty)$. Results of the shift of the transition temperature obtained in this way are plotted in Fig.(7) versus inverse volume. The shift critical exponent obtained from a fit to the form: $\tau_T(V) \sim V^{-\lambda}$, is: $\lambda = 0.876 \pm 0.041$.

4.2.3. The Shift from the Fourth Binder Cumulant

Another way for locating $T_c(V)$ is to consider the fourth order cumulant of the order parameter proposed in [12] and defined as:

$$B_4(T, V) = 1 - \frac{\langle \mathfrak{h}^4(T, V) \rangle}{3 \langle \mathfrak{h}^2(T, V) \rangle^2}, \quad (23)$$

which presents a minimum value at an effective transition temperature whose shift from the true transition temperature is of order V^{-1} for a first order transition. This cumulant has been proven to be a suitable indicator of the order of the transition in a finite volume, since a nonvanishing value of $(\frac{2}{3} - B_4^{\min})$ signals a first order transition, whereas for a second order transition, $\lim_{V \rightarrow \infty} (\frac{2}{3} - B_4) = 0$ even at the transition point. Indeed, for a first order transition the quantity $\lim_{V \rightarrow \infty} (\frac{2}{3} - B_4)$ vanishes at all points apart from the transition point, and $(\frac{2}{3} - B_4^{\min})$ measures the latent heat [12, 13, 15, 16].

The expression of $B_4(T, V)$ as function of the integral terms, for this case of the deconfinement transition, is after calculation:

$$B_4(T, V) = 1 - \frac{(L_{11} - L_{01})(24(L_{15} - L_{05} - L_{04}) - 12L_{03} - 4L_{02} - L_{01})}{3(2L_{13} - 2L_{03} - 2L_{02} - L_{01})^2}. \quad (24)$$

Fig.(8-left) illustrates the variations of the fourth cumulant of the order parameter with temperature for various volumes, and shows that the locations of the minima in finite sizes $T_{\min}(V)$ are shifted to higher values from $T_c(\infty)$. Data of the shift of the transition temperature obtained in this way are plotted in Fig.(8-right) versus inverse volume, and the scaling shift critical exponent obtained from a fit to the form: $\tau'_T(V) = T_{\min}(V) - T_c(\infty) \sim V^{-\lambda'}$, is: $\lambda' = 0.883 \pm 0.043$.

4.2.4. Parametrization of the Order Parameter and the Susceptibility

Within the model used in this work, the order parameter in the limit of infinite volume being equal to 1 below the transition temperature and zero above, it can then be expressed in a simple way using the Heaviside step-function as:

$$\langle \mathfrak{h}(T, V \rightarrow \infty) \rangle = 1 - \Theta(T - T_c(\infty)). \quad (25)$$

Such a parametrization has been used in [17], for a similar case of a system of coexisting hadronic matter and QGP phases. Using one of the known mathematical representations of the smoothed step function $\Theta(T - T_c)$, the order parameter may then be expressed as:

$$\langle \mathfrak{h}(T, V) \rangle = \frac{1}{2} \left(1 - \tanh \left(\frac{T - T_c(V)}{\Gamma_T(V)} \right) \right), \quad (26)$$

where T_c is the effective transition temperature and Γ_T the half-width of the rounded transition region, which leads to the susceptibility expression :

$$\chi(T, V) = \frac{-1}{2\Gamma_T(V) \cosh^2 \left(\frac{T - T_c(V)}{\Gamma_T(V)} \right)}. \quad (27)$$

The parametrisation choice (26) is the most accepted physically, and it can be understood phenomenologically in the context of the Double Gaussian Peaks model where the obtained expressions of the order parameter and the susceptibility are very similar to (26) and (27) [5, 18].

An illustration of such parametrizations of the order parameter at the volume $V = 4000 fm^3$, and the susceptibility at the volume $V = 900 fm^3$ are presented in Figs.(9-left) and (9-right) respectively, and the parameters $T_c(V)$ and $\Gamma_T(V)$ obtained from each fit are given.

The results for the width of the transition region $\delta T^{fit(1)}(V)$ and the shift of the transition temperature $\tau_T^{fit(1)}(V)$ from the parametrization of the order parameter are plotted with inverse volume in Fig.(10) and those from the parametrization of the susceptibility, $\delta T^{fit(2)}(V)$ and $\tau_T^{fit(2)}(V)$ in Fig.(11). Their fits to power law forms: $\tau_T^{fit(1)}(V) \sim V^{-\lambda_1}$, $\tau_T^{fit(2)}(V) \sim V^{-\lambda_2}$, $\delta T^{fit(1)}(V) \sim V^{-\theta_1}$ and $\delta T^{fit(2)}(V) \sim V^{-\theta_2}$ give: $\lambda_1 = 0.830 \pm 0.013$, $\lambda_2 = 0.857 \pm 0.006$, $\theta_1 = 0.990 \pm 0.015$ and $\theta_2 = 1.032 \pm 0.003$.

5. CONCLUSION

Our work has shown the influence of the finiteness of the system size on the behavior of some response functions in the vicinity of the transition point. The sharp transition observed in the thermodynamical limit, signaled by discontinuities in the order parameter and in the energy density at a transition temperature $T_c(\infty)$, is rounded off in finite volumes, and the variations of these thermodynamic quantities are perfectly smooth on the hole range of temperature. The delta function singularities appearing in the first derivatives of these discontinuous quantities, i.e., in the susceptibility and specific heat density, are then smeared out into finite peaks of widths $\delta T(V)$. The maxima of these peaks occur at effective transition temperatures $T_c(V)$ shifted away from the true transition temperature $T_c(\infty)$. A FSS analysis of the behavior of the maxima of the rounded peaks of the susceptibility $\chi_T^{\max}(V)$ and the specific heat density $c_T^{\max}(V)$, the width of the transition region $\delta T(V)$, and the shift of the effective transition temperature relative to the true one $\tau_T(V) = T_c(V) - T_c(\infty)$, shows their power-law variations with the volume characterized by the scaling critical exponents γ , α , θ , and λ respectively. Numerical results for these scaling exponents are obtained and are in good agreement with our analytical results: $\gamma = \alpha = \theta = \lambda = 1$ obtained in [19], except for the shift critical exponent which slightly deflects from the analytical value 1. This may be due to the difficulty of locating accurately the peaks of χ , c and B_4 , especially in the case of large volumes for which the peaks become very sharp. However, a first estimate of the scaling critical exponents for the thermal DPT within this model has been obtained, and our result expressing the equality between all scaling exponents and the space dimensionality is a consequence of the singularity characterizing a first order phase transition and agrees very well with the predictions of other FSS theoretical approaches [20] and with the results of both lattice QCD [21] and Monte Carlo models calculations.

[1] C. N. Yang and T. D. Lee, Phys. Rev. **87** (1952) 404; Phys. Rev. **87** (1952) 410.

[2] J. Imry, Phys. Rev. B **21** (1980) 2042.

[3] K. Binder and D. P. Landau, Phys. Rev. B **30** (1984) 1477.

[4] C. Spieles, H. Stöcker and C. Greiner, Phys. Rev. C **57** (1998) 908.

[5] H. Meyer-Ortmanns, Rev. Mod. Phys. **68** (1996) 473.

[6] K. Redlich and L. Turko, Z. Phys. C **5** (1980) 201; L. Turko, Phys. Lett. **104B** (1981) 153.

[7] H.-Th. Elze, W. Greiner and J. Rafelski, Phys. Lett. **124B** (1983) 515; Zeit. Phys. C **24** (1984) 361; H.-Th. Elze and W. Greiner, Phys. Lett. **179B** (1986) 385.

- [8] A. Tounsi, J. Letessier and J. Rafelski, hep-ph/9811290.
- [9] M. G. Mustafa, D. K. Srivastava and B. Sinha, Eur. Phys. J. C **5** (1998) 711; nucl-th/9712014.
- [10] G. Yezza, Magister thesis in theoretical physics, Ecole Normale Supérieure-Kouba, Algiers (March 2002).
- [11] M. E. Fisher and A. N. Berker, Phys. Rev. B **26** (1982) 2507.
- [12] M. S. Challa, D. P. Landau and K. Binder, Phys. Rev. B **34** (1986) 1841.
- [13] K. Binder and D. W. Heermann, *Monte Carlo Simulations in Statistical Physics*, (Springer-Verlag, 1988, 2nd ed. 2002).
- [14] M. Henkel, *Conformal Invariance and Critical Phenomena*, Springer Verlag (1999).
- [15] K. Binder, Rep. Prog. Phys. **60** (1997) 487.
- [16] D. P. Landau and K. Binder, *A Guide to Monte Carlo Simulation in Statistical Physics*, (Cambridge University Press, 2000).
- [17] J. P. Blaizot and J. Y. Ollitrault, Phys. Rev. **D36** (1987) 916.
- [18] K. Binder, Phys. Rev. Lett. **47** (1981) 693; Zeit. Phys. B **43** (1981) 119; K. Binder & D. P. Landau, Phys. Rev. B **30** (1984) 1477.
- [19] M. Ladrem, A. Ait-El-Djoudi and G. Yezza, communication at the international conference ‘Quark Confinement and the Hadron spectrum’, held in Gargnano-Italy from 10 to 14 September 2002.
- [20] J. G. Brankov, D. M. Danchev and N. S. Tonchev, *Theory of Critical Phenomena in Finite-Size Systems - Scaling and Quantum Effects*, (World Scientific, 2000).
- [21] B. Beinlich, F. Karsch, E. Laermann and A. Peikert, Eur. Phys. J. C **6** (1999) 133.

Figure Captions

Fig. 1: Temperature variation of the order parameter (top) and the energy density normalized by T^4 (bottom) at $\mu = 0$, for different system volumes.

Fig. 2: Plot of (Left) the susceptibility $\chi(T, V)$ and (Right) the specific heat density $c(T, V)$, versus temperature for different system volumes.

Fig. 3: Plot of the second derivative of the order parameter $\langle \mathfrak{h}(T, V) \rangle'' = \frac{\partial^2 \langle \mathfrak{h}(T, V) \rangle}{\partial T^2}$ versus temperature for different system volumes.

Fig. 4: Illustration of the finite size behavior of the susceptibility $\chi(T, V)$, the specific heat density $c(T, V)$ and the second derivative of the order parameter $\partial\chi/\partial T$.

Fig. 5: Variation of (Left) the susceptibility maxima $|\chi_T|^{\max}(V)$ and (Right) the specific heat density maxima $c_T^{\max}(V)$ with volume.

Fig. 6: Variation of the width of the temperature region over which the transition is smeared $\delta T(V)$ with inverse volume.

Fig. 7: Variation of the shift of the transition temperature $\tau_T(V)$ (from the maxima of $\chi(T, V)$ and $c(T, V)$) with inverse volume.

Fig. 8: (Left) Plot of the fourth Binder cumulant $B_4(T, V)$ versus temperature for different system volumes, and (Right) variation of the shift of the transition temperature $\tau'_T(V)$ (from the minimum of $B_4(T, V)$) with inverse volume.

Fig. 9: Illustration of the fits of the order parameter to the form (26) at the volume $V = 4000 fm^3$, and of the susceptibility to the form (27) at the volume $V = 900 fm^3$.

Fig. 10: Variations of (Left) the width of the transition region $\delta T^{fit(1)}(V)$, and (Right) the shift of the transition temperature $\tau_T^{fit(1)}(V)$, obtained from the parametrization in eq. (26), with inverse volume.

Fig. 11: Variations of (Left) the width of the transition region $\delta T^{fit(2)}(V)$, and (Right) the shift of the transition temperature $\tau_T^{fit(2)}(V)$, obtained from the parametrization in eq. (27), with inverse volume.

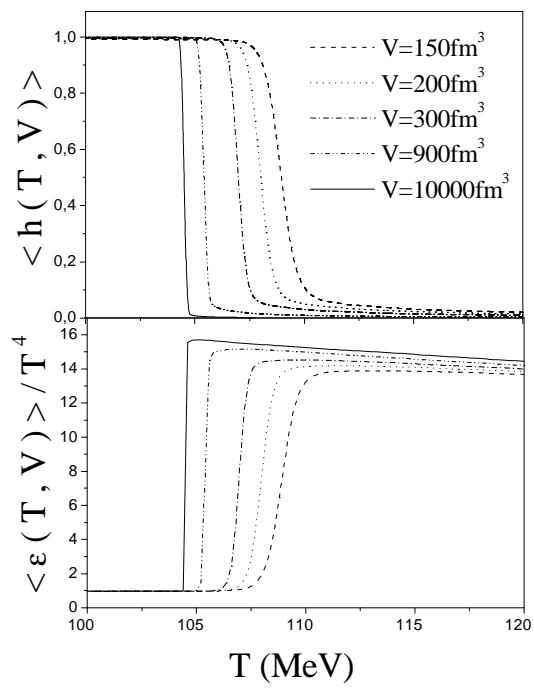


Fig. 1

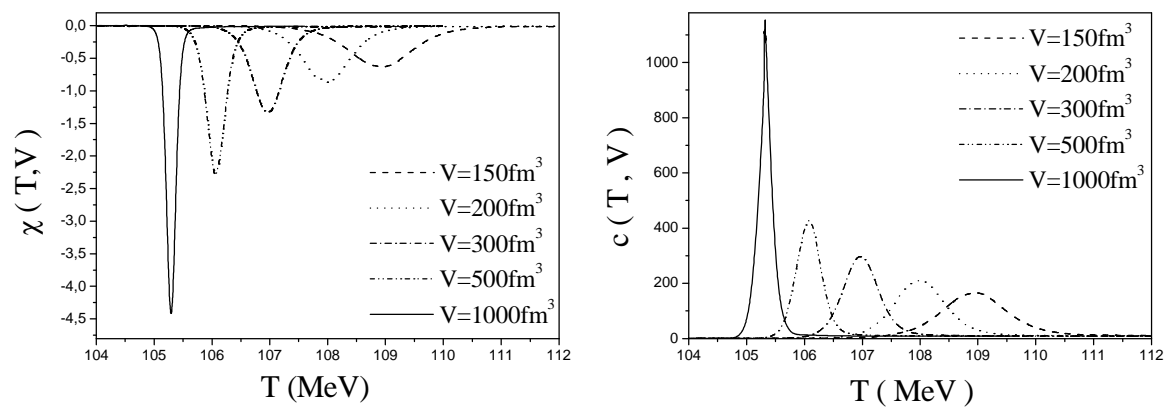


Fig. 2

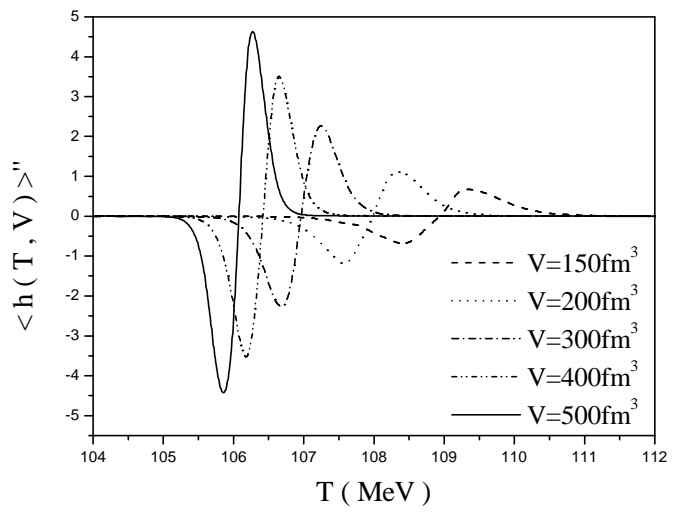


Fig. 3

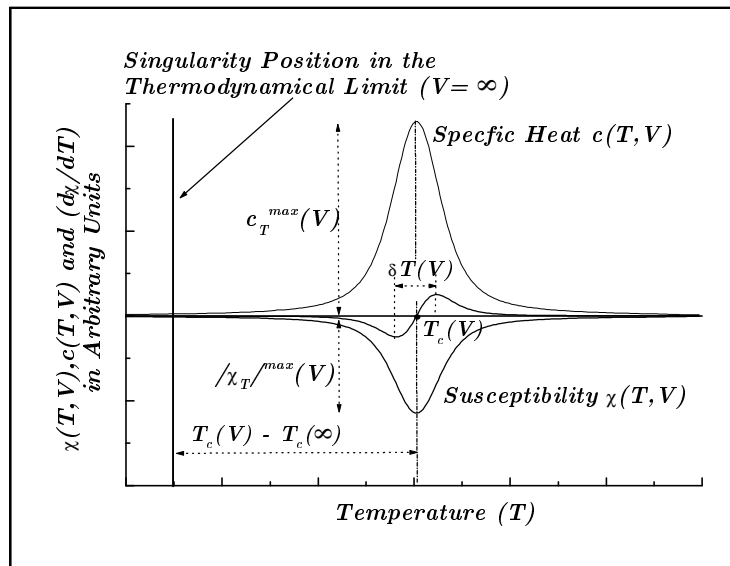


Fig. 4

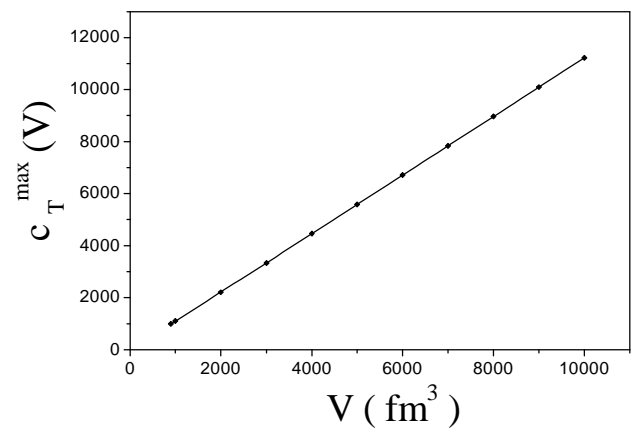
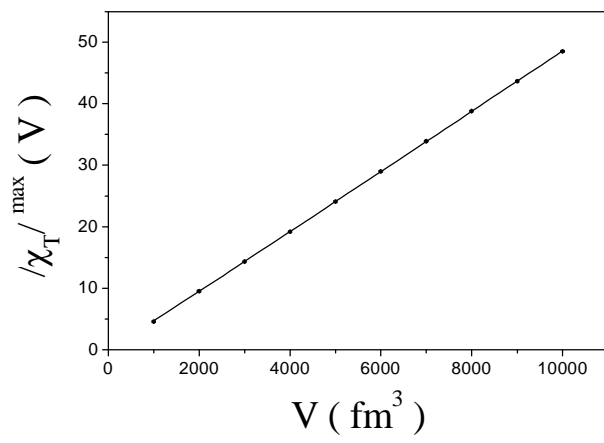


Fig. 5

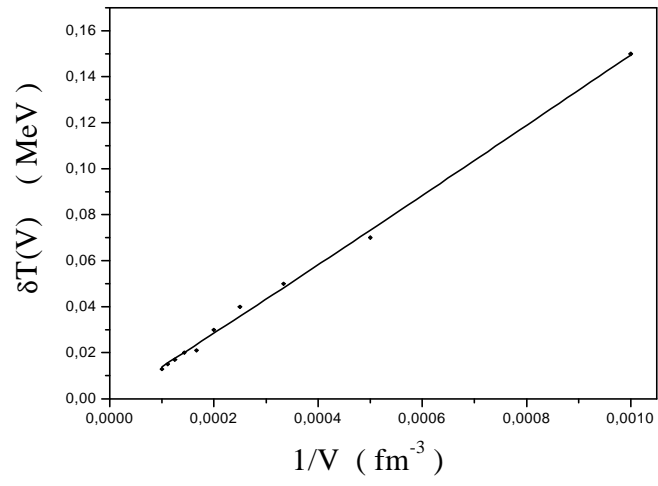


Fig. 6

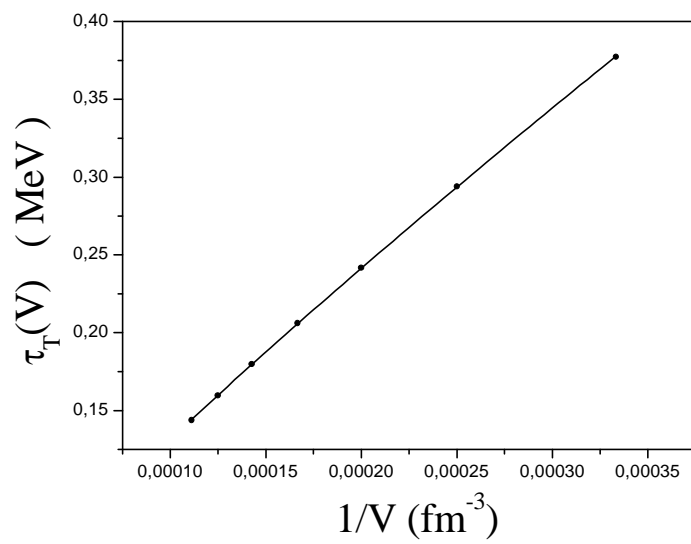


Fig. 7

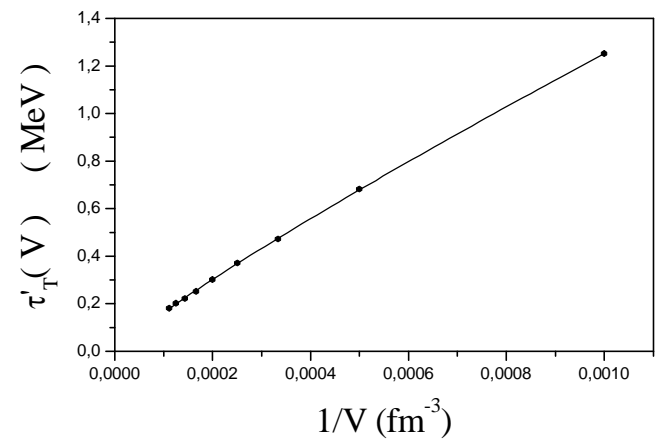
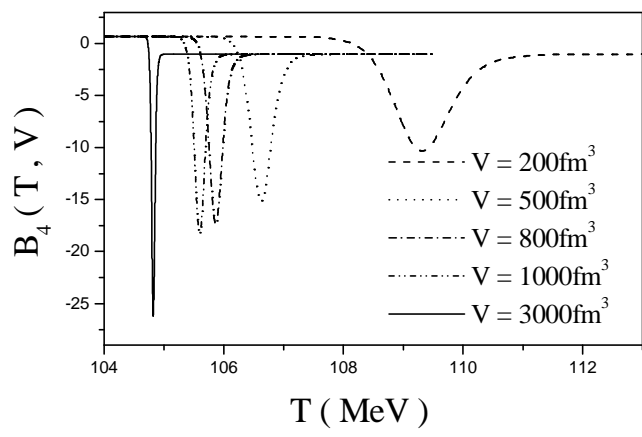


Fig. 8

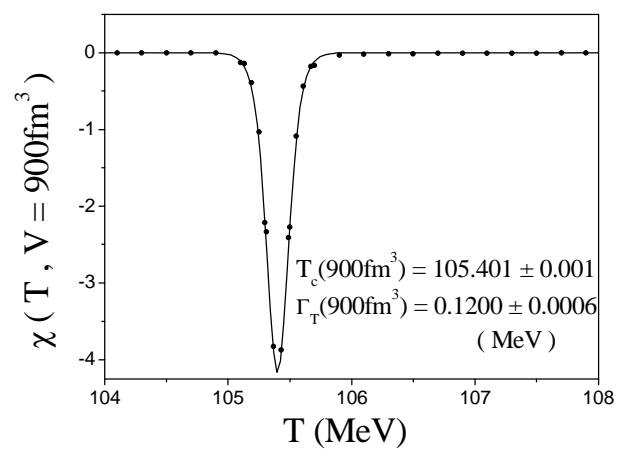
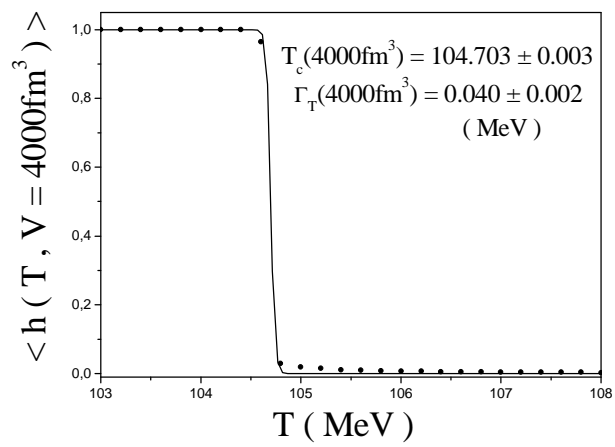


Fig. 9

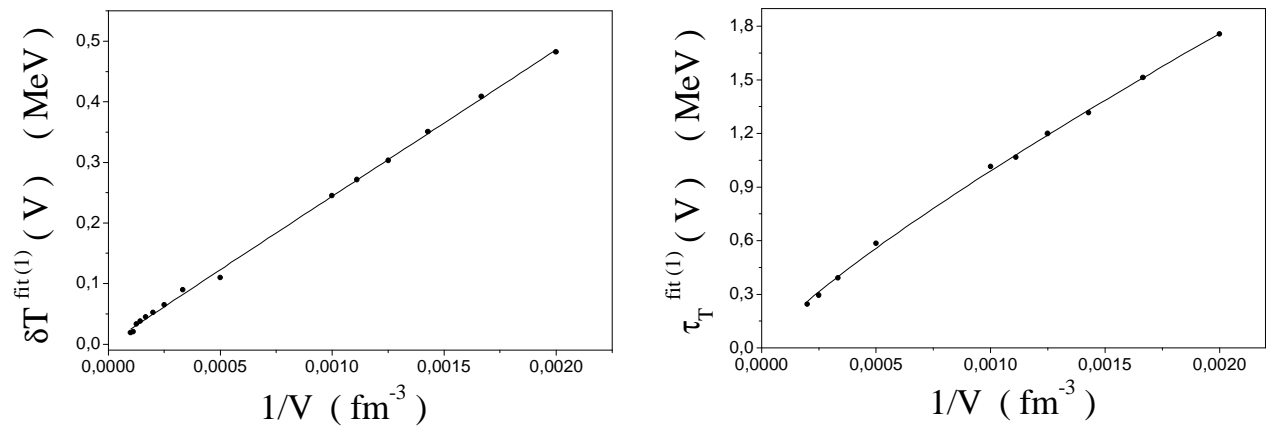


Fig. 10

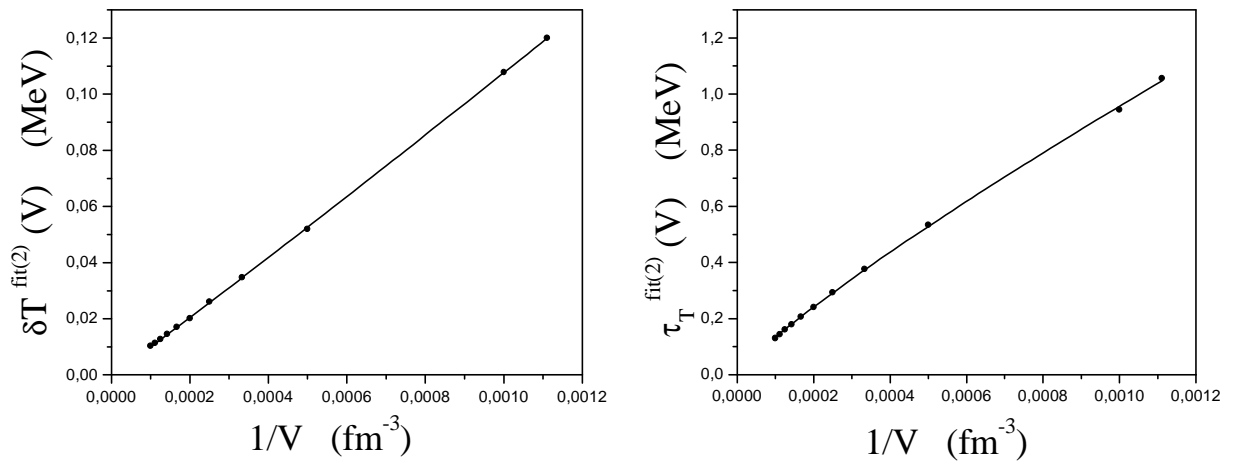


Fig. 11